

## CHAPTER IV

### RESULTS AND DISCUSSION

In many fermentation systems, the use of adsorption or entrapment technique alone might be not sufficient for cell immobilization because the problems of cell detachment, diffusion limitations of nutrients and metabolites and gel degradation [6, 21, 32]. In order to improving the drawback of immobilization for ethanol fermentation, *Saccharomyces cerevisiae* M30 immobilized by  $\gamma$  – alumina doped alginate gel (AEC) was developed as a new carrier by the integration of adsorption and entrapment techniques [6]. *Saccharomyces cerevisiae* could be adsorbed on  $\gamma$  –  $\text{Al}_2\text{O}_3$  by electrostatic attraction in wide pH range 3-6.5 [5]. In the previous study, immobilization of cells was investigated using two general steps. The first was the adsorption of cells onto the surface of  $\gamma$ - $\text{Al}_2\text{O}_3$ . The second was the entrapment of  $\gamma$ - $\text{Al}_2\text{O}_3$ -cells in Ca-alginate matrix. The ethanol fermentation was performed using suspended cell (SC) culture, immobilized cells on  $\gamma$ - $\text{Al}_2\text{O}_3$  (AC) culture and adsorption a  $\gamma$ - $\text{Al}_2\text{O}_3$ -entrapment alginate (AEC) culture in a single batch and a 4-cycle repeated batch. From the finding of J. Pullsirisombat (2007), AEC carrier ( $\emptyset$  3 mm) had a good potential as a carrier for yeast cell immobilization. There were several advantages, including high ethanol production, high density of biomass, more stable than suspension cell culture and good potential for reusability [6].

This work attempts to develop and promote AEC carrier for using in continuous ethanol fermentation process. The experiments were divided into 3 parts. Firstly, prestudying the effect of the integration of  $\text{Al}_2\text{O}_3$  in alginate bead on the cell activity. The cells activity of AEC culture was compared with that of the system of suspension cell and immobilized cell in alginate bead. Secondly, the effect of the controlled parameters in the bead such as the bead diameter, Na-alginate concentration and  $\text{Al}_2\text{O}_3$  concentration on ethanol fermentation were investigated in batch fermentation. Thirdly, studying the performance of ethanol production by using AEC carrier in packed bed reactor. The

optimum condition from the previous batch system was applied for the packed bed reactor. The effect of dilution rate was investigated in continuous fermentation.

#### 4.1 Prestudy for the effect of alumina ( $\text{Al}_2\text{O}_3$ ) in alginate bead on immobilization of *S. cerevisiae* M30

The system of cell immobilization by entrapment in alginate bead was compared with that of adsorption on  $\text{Al}_2\text{O}_3$  and then the combination of entrapment in alginate bead. The fermentation was carried out with 225 g/l of initial sugar concentration from sugar cane molasses as a carbon source for *S.cerevisiae* M30. Batch fermentations were performed in the shaking incubator at 150 rpm, 33°C for 72 hours. The samples were harvested every 8 hours for cell, sugar and ethanol analyses. Three cultures were evaluated in this fermentation. Labels of each culture were given Table 4.1.

**Table 4.1** List of samples and labels for this study

Sample's Name	Label
Suspended cells culture	SC
Entrapment in alginate culture	EC
Adsorption $\text{Al}_2\text{O}_3$ -Entrapment alginate culture	AEC

The effect of  $\text{Al}_2\text{O}_3$  in the cell carrier was studied by the comparison of cell activities in EC and AEC carriers, in which the bead diameter was varied from 4 mm to 6 mm. The activities of the immobilized cells were also compared to the systems of free cells (SC). In preparation of immobilized cells, 1.5% (w/v) of Na-alginate was used for EC carrier, 1.5% (w/v) of Na-alginate and 5% (w/v of alginate) of  $\text{Al}_2\text{O}_3$  were used for AEC carrier. The results of the fermentation are summarized in Table 4.2

**Table 4.2** Yield and end products of batch ethanol fermentation for 72 hours using the cultures of SC, EC and AEC

System	Ethanol concentration (g/l)	Residual sugar concentration (g/l)	Free cell (g/l)	Immobilized cell (g/l)	Y <sub>I</sub> (%)	Y <sub>P/S</sub> (%)
SC	85.07	33.62	3.74	-	-	44.42
Ø 4 mm						
EC	89.52	21.44	0.76	3.26	81.09	43.95
AEC	91.67	20.29	0.81	3.54	81.38	44.75
Ø 6 mm						
EC	81.93	35.84	0.91	2.96	76.49	43.28
AEC	86.76	28.38	0.76	3.36	81.55	44.10

At the end of the fermentation, the total cell concentration of AEC<sub>4mm</sub> (4.35 g/l), AEC<sub>6mm</sub> (4.12 g/l), EC<sub>4mm</sub> (4.02 g/l) and EC<sub>6mm</sub> (3.87 g/l) were obtained, which were slightly higher than that of SC (3.74 g/l). The immobilization yields of the AEC<sub>4mm</sub>, AEC<sub>6mm</sub>, EC<sub>4mm</sub> and EC<sub>6mm</sub> were 81.38%, 81.55%, 81.09% and 76.49% respectively. Final cell concentration inside immobilized cell carriers (EC and AEC) was much higher than the initial cell (inoculum). This was indicated that yeast cells could be grown inside the immobilized cell carriers. At the end of fermentation, the immobilized cell carriers were heavier, darker, and bigger than the initial carriers. Therefore, the immobilized cells carriers (AEC and EC) could be promoted the growth of *S.cerevisiae* M30. In the previous studies, the matrix of the immobilized cells carriers can protect yeast by fortification from toxins and inhibitor [3, 32]. The total cell concentrations and immobilization yields of AEC carrier of both sizes were relatively higher than that of EC carrier. It was demonstrated that Al<sub>2</sub>O<sub>3</sub> has a positive effect on the growth of *S.cerevisiae* M30. This was similar to the finding of Kana et al. (1989) who reported that  $\gamma$ - Al<sub>2</sub>O<sub>3</sub> was a good supporter of ethanol fermentation because of the electrostatic attraction between  $\gamma$ - Al<sub>2</sub>O<sub>3</sub> particles and yeast cells [5]. The adsorption of cells on the surface of Al<sub>2</sub>O<sub>3</sub>

should be due to high positive charge density on the surface of the carrier and negative charge on the yeast cell wall. Such attachment may depend not only on electrostatic forces, but also on chemical bonds between carboxyl groups, amino groups and hydroxyl groups of the cell wall and  $Al^{3+}$  ions [33]. The slightly lower immobilization yield of EC carrier at the bigger size diameter bead was as a result of the increase in gel degradation followed by cell detachment which was found related to the bead diameter in this case.

As shown in Figure 4.1 and 4.2, the concentration of sugar gradually decreased while the ethanol concentration increased for duration of 72 hours. The final residual sugar concentration of SC, EC<sub>4mm</sub>, EC<sub>6mm</sub>, AEC<sub>4mm</sub> and AEC<sub>6mm</sub> system were 33.62, 21.44, 35.84, 20.29 and 28.38 g/l, respectively and the final ethanol concentration were 85.07, 89.52, 81.93, 91.67 and 86.76 g/l, respectively ( $Y_{P/S}$  44.42%, 43.95%, 43.28%, 44.75% and 44.10%, respectively).

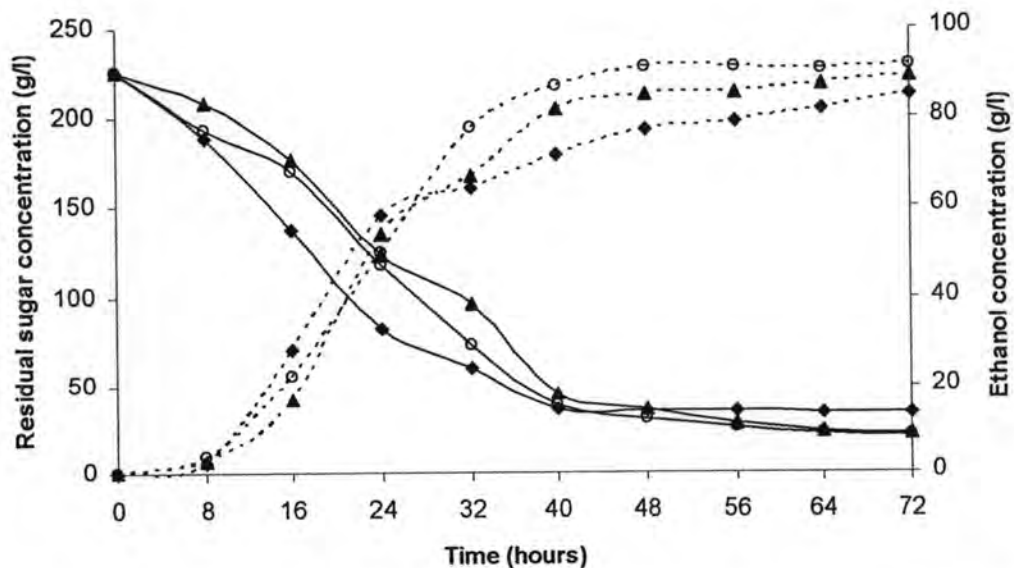


**Figure 4.1** Residual sugar concentration and ethanol concentration profile in fermentation of 4 mm bead diameter size; Residual sugar concentration (solid lines) and Ethanol concentration (dash lines);  $\blacklozenge$ , SC;  $\blacktriangle$ , EC and  $\circ$ , AEC

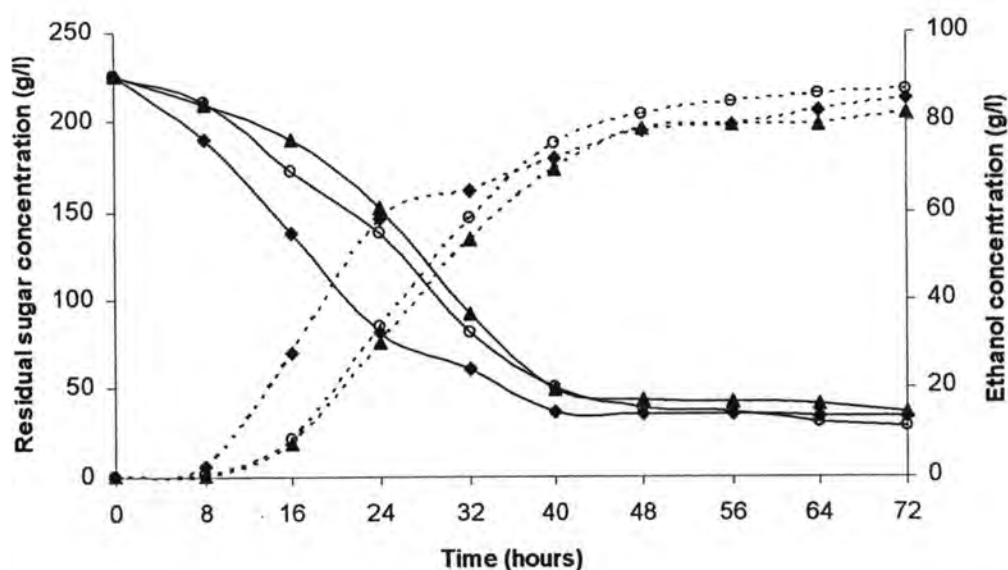


**Figure 4.2** Residual sugar concentration and ethanol concentration profile in fermentation of 6 mm bead diameter size; Residual sugar concentration (solid lines) and Ethanol concentration (dash lines); ◆, SC; ▲, EC and ○, AEC

A comparison of experimental results, showed that sugar consumption and ethanol production trend of immobilized cell carrier (EC and AEC) in 4 mm diameter system was initially lower than that of SC system for duration of 24 hours but became higher after that. The final ethanol concentration of SC system was lower than AEC<sub>4mm</sub>, EC<sub>4mm</sub>, and AEC<sub>6mm</sub> system but higher than EC<sub>6mm</sub> system. The cell activities of AEC<sub>4mm</sub>, EC<sub>4mm</sub>, and AEC<sub>6mm</sub> system were better than SC system which might be attributable to the negative effect of high ethanol concentration on cell activity and viability in SC system. The ability of cells to grow in an immobilized state made it possible for cell regeneration and product formation under hostile conditions such as high ethanol concentration [32]. This phenomenon can be attributed to cell encapsulation by a protective layer of gel material or to modified fatty acid concentration in cell membranes due to oxygen diffusion limitations. Osmotic stress caused by the immobilization techniques was found to lead to an intracellular production of pressure regulating compounds such as polyols, which lead to decreased water activity and consequently higher tolerance to toxic compounds [34].

The structure and size of cell carrier are important factors affected cell activities. From the comparison of diameter sizes, the increasing of bead diameter from 4 mm to 6 mm resulted in the decrease of ethanol concentration at 5.4% in the AEC carrier system and 8.5% in the EC carrier system. While the immobilization yield ( $Y_1$ ) of the AEC remained constant at around 81%, the  $Y_1$  of the EC dropped from 81% to 76% with the increase of the diameter from 4 to 6 mm. The decrease of ethanol production and immobilization yield ( $Y_1$ ) of the EC carrier at  $\varnothing$  6 mm could be due to the drop of cell growth and metabolite inside the carrier. At large size, accessibility of the nutrient into inner portion of the carrier might become the limiting factor for cell activities, especially for the carrier with the dense structure. This result revealed that the mass transfer limitation through the porous structure of the AEC carrier might be less severe than that of the EC carrier.

A series of SEM images were taken to provide visual description and information of fermentation system. To study the characteristic of cell adsorption, the sample of adsorbed cells on  $\text{Al}_2\text{O}_3$  was prepared by culture cells in preculture medium for 24 hours which was called the preculture or first immobilization step. Figure 4.3 presented a picture of cell adsorption on  $\text{Al}_2\text{O}_3$ . As seen from the picture, *S.cerevisiae* M30 could grow and link with  $\text{Al}_2\text{O}_3$  in form of network structure. However, this attachment force was not enough for protect cell detachment due to shear force during the batch shaking flask fermentation. This problem was solved by entrapped the adsorbed cells on  $\text{Al}_2\text{O}_3$  with alginate. The attachment of cells on  $\text{Al}_2\text{O}_3$  constructed the network of cell and  $\text{Al}_2\text{O}_3$  inside the gel carrier. This network would increase the porosity and strength of carrier.

The overall view of AEC ( $\varnothing$  6 mm) and EC ( $\varnothing$  2 mm – the result from the experiment of R. Busdianto (2006) [21]) at the end of fermentation was shown in Figure 4.4 and 4.5. These pictures showed that yeast cells in AEC and EC were protected by film of alginate. Nevertheless, some cells may escape from holes or scars on the surface of the carrier. The surface of EC (Figure 4.6) was not as smooth as AEC (Figure 4.7) because the majority of yeast grown at the outer part of EC. The cross sectional view of EC was provided in Figure 4.9, small amount of cells in the inner part of the bead were

observed because of the gel in the center of the bead was tight with less porosity. The preference of the cells to live near the surface rather than deep inside the bead had also been reported by Najafpour (2004). High accessibility to food as a consequence of better mass transfer near the surface is proposed as the main driving force [19]. Nonetheless, the intense growth might be the cause of cell leakage. As more cells were grown near the surface, the film of gel at the surface expands and becomes thinner. SEM observation of AEC cross section in Figure 4.8 demonstrated that yeast could grow well inside the structure of AEC carrier. The cells appeared healthy and retained their normal oval shape as confirmed by close look image in Figure 4.10. This confirmed that the yeast could gain access to substrate needed for growth even though they were located deep inside the carrier. It suggested that there was not strong mass transfer limitation inside the AEC bead. The network of  $\text{Al}_2\text{O}_3$  and cell inside the bead might create microporous structure that could enhance the mass transfer across the matrix. Thus, AEC structure might be responsible for the high cell adsorption and improved mass transportation.

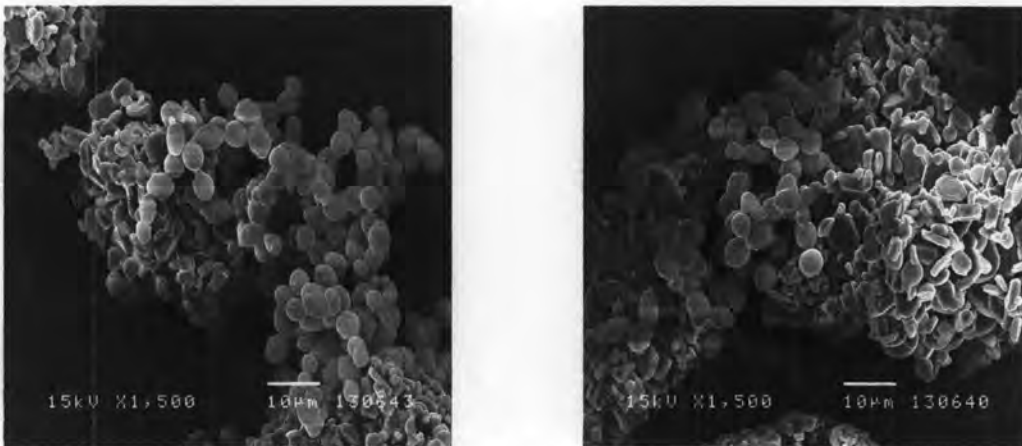


**Figure 4.3** Adsorbed cells on  $\text{Al}_2\text{O}_3$  (x1500)

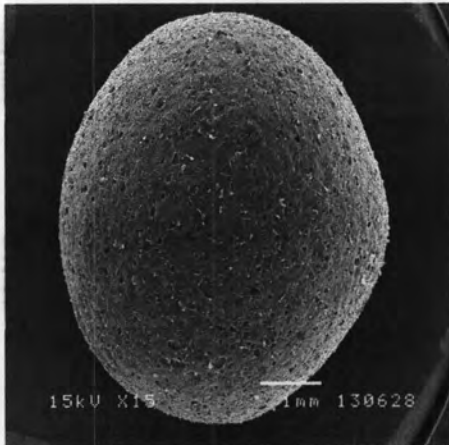


**Figure 4.4** The overall view of AEC<sub>6mm</sub>  
(x15)

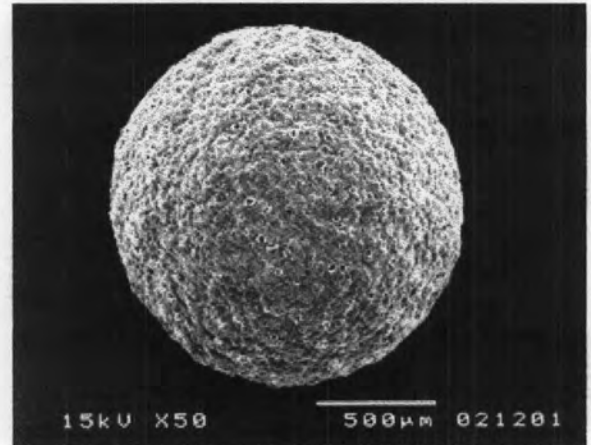


**Figure 4.5** The overall view of EC<sub>2mm</sub>  
R. Busdianto [21] (x50)

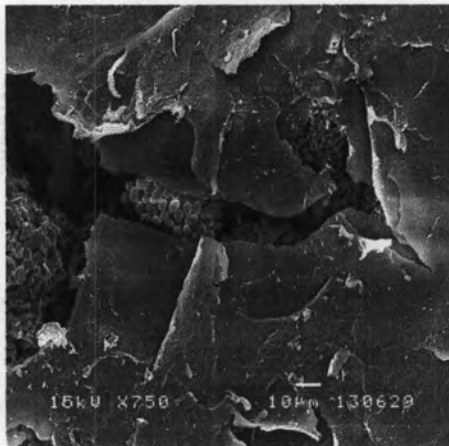


**Figure 4.6** Surface of AEC<sub>6mm</sub>  
(x750)

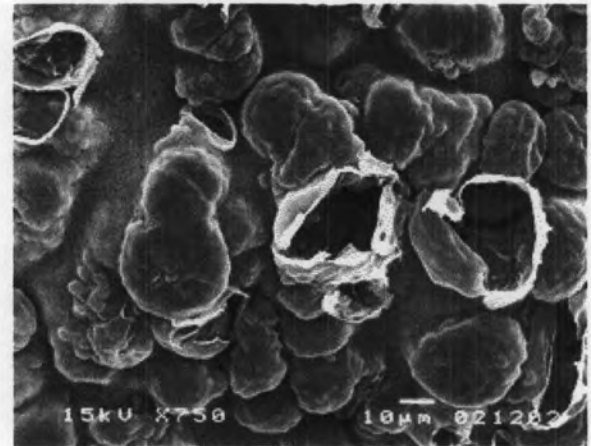


**Figure 4.7** Surface of EC<sub>2mm</sub>  
R. Busdianto [21] (x750)



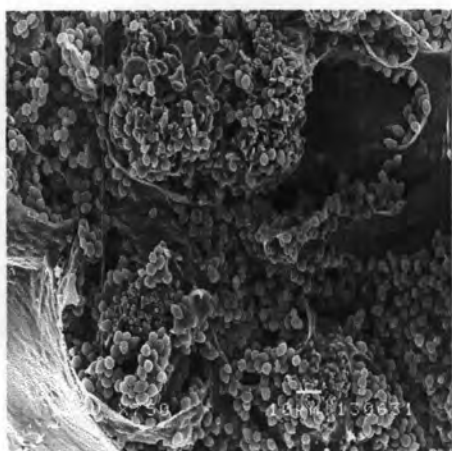


**Figure 4.8** Cross section of AEC<sub>6 mm</sub>  
(x750)

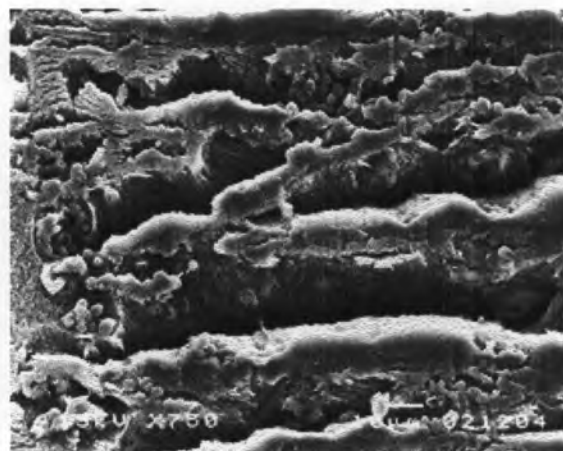


**Figure 4.9** Cross section of EC<sub>2 mm</sub>  
R. Busdianto [21] (x750)

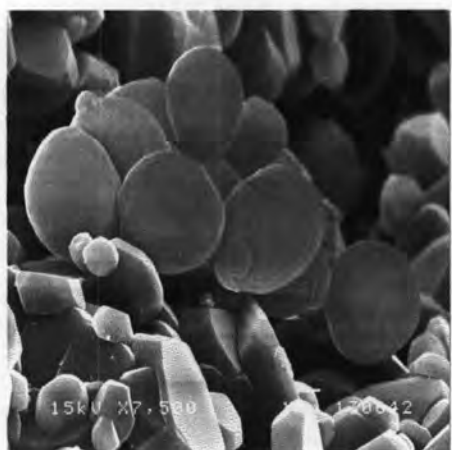


**Figure 4.10** Close look on AEC<sub>6 mm</sub>  
cross section (x7500)

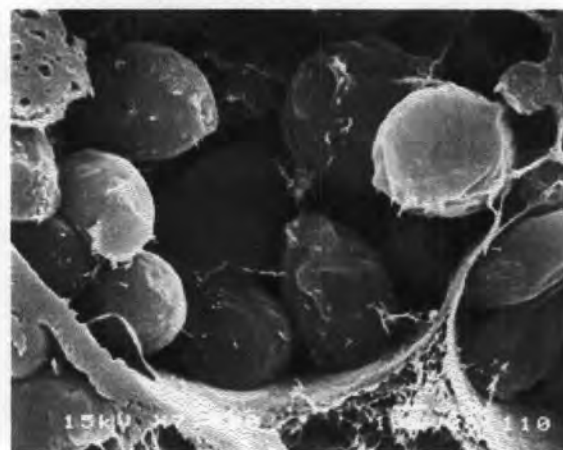


**Figure 4.11** Close look on EC<sub>2 mm</sub>  
cross section R. Busdianto [20] (x7500)

Alumina doped alginate gel (AEC) carrier behaved as an effective immobilized cell carrier, resulting in improved cell density and ethanol productivity. To increase the efficiency of AEC carrier, the effect of important parameters such as bead diameter size, alginate concentration and Al<sub>2</sub>O<sub>3</sub> concentration on the ethanol fermentation were further investigated.

## 4.2 Effect of bead diameter

In immobilized microorganism systems, diffusion resistances could be eliminated by using small particles, a high degree of turbulence around the particles and high substrate concentrations. For maximum conversion rates, the particle size should be as small as possible within the constraints of particle integrity, resistance to compression and the nature of the particle recovery systems [35]. From a previous work, by Göksungur et al. (2001), ethanol production from beet molasses using Ca-alginate immobilized yeast cells in a packed bed reactor increased as bead diameter decreased [26]. This result attributed to the fact that a given volume of larger bead has less surface area available for mass transfer of substrate into and through the bead.

In order to determine the effect of bead diameter on ethanol production of AEC carrier, beads with diameter of 2 mm, 4 mm and 6 mm (Figure 4.12) were prepared by using different size of auto pipette tip (1 ml, 5 ml and 10 ml, respectively) with 1.5% (w/v) of Na-alginate and 5% (w/v of alginate) of  $Al_2O_3$ . The ethanol production in batch shaking flask was performed with initial sugar concentration of 225 g/l. As shown in Figure 4.13, during 16 - 40 hours of cultivation, the ethanol production and sugar consumption of 2 mm bead diameter system was higher than those of 4 mm and 6 mm bead diameter systems. This could be indicated that an increase in surface volume ratio caused a mass transfer resistance in this time period. However, the final ethanol concentration of 4 mm and 6 mm bead diameter systems reached to the similar level of that from 2 mm bead diameter system. The consumption of sugar for the three systems reached steady state after 48 hours. The ethanol concentrations profiles were corresponded to sugar concentration profiles. It was proposed that residual sugars available at this level might be the unfermented sugars for the yeast cell.

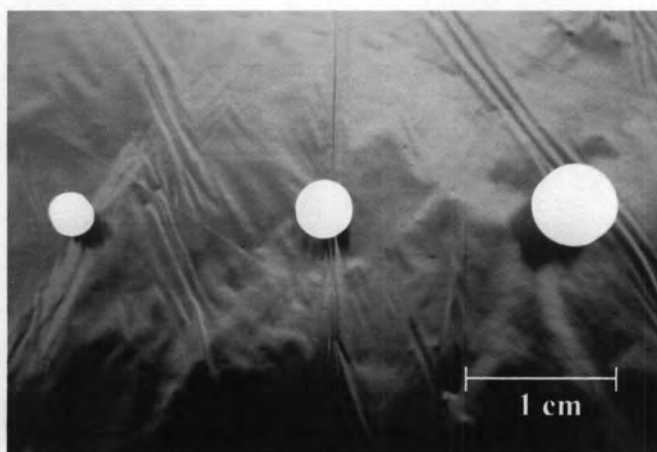


**Figure 4.12** AEC carriers with bead diameter of 2 mm, 4 mm and 6 mm

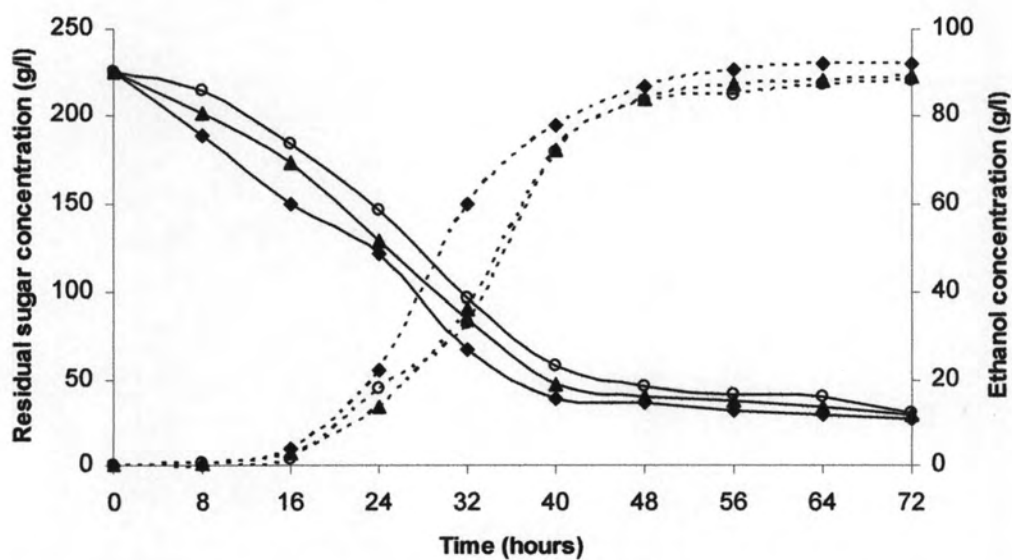


**Figure 4.13** Effect of bead diameter on residual sugar concentration and ethanol concentration of AEC carrier; Residual sugar concentration (solid lines) and Ethanol concentration (dash lines); ◆,  $\varnothing$  2mm; ▲,  $\varnothing$  4 mm and ○,  $\varnothing$  6 mm

**Table 4.3** Yield and end products of batch ethanol fermentation for 72 hours using the cultures of AEC carrier with bead diameter of 2 mm, 4 mm and 6 mm

<b>Bead diameter (mm)</b>	<b>Ethanol concentration (g/l)</b>	<b>Residual sugar concentration (g/l)</b>	<b>Free cell (g/l)</b>	<b>Immobilized cell (g/l)</b>	<b>Y<sub>I</sub> (%)</b>	<b>Y<sub>P/S</sub> (%)</b>
2	92.03	27.58	0.86	4.19	82.94	46.60
4	89.30	29.31	0.79	3.68	82.28	45.62
6	88.00	30.46	0.73	3.50	82.84	45.22

The relationship between cell concentration, sugar utilization and ethanol formation of AEC carrier with bead diameter of 2 mm, 4 mm and 6 mm were shown in Table 4.3. The highest ethanol concentration (92.03 g/l) was obtained from the smallest particle ( $\varnothing$  2 mm AEC carrier). An increase in bead diameter to 4 mm resulted in a slightly decrease of ethanol concentration to 89.30 g/l or 2.96% decreasing from that of 2 mm AEC carrier. A further increase in bead diameter to 6 mm resulted in a decrease of ethanol concentration to 88.00 g/l or 4.38% decreasing from that of 2 mm AEC carrier and 1.46% decreasing from that of 4 mm AEC carrier. The production yields of bead with diameter of 2 mm, 4 mm and 6 mm were 46.60%, 45.62% and 45.22%, respectively. From this result, ethanol formation and production yield of 6 mm bead diameter system was slightly different from those of 2 mm bead diameter system. Therefore, for AEC carrier in the range of 2 – 6 mm bead diameter, the internal diffusion slightly affected the cell activities.

As shown in Figure 4.14, the immobilized cell concentration of 2 mm bead diameter system was relatively higher than that of 4 mm and 6 mm bead diameter systems. At the end of the fermentation (Table 4.3), the highest immobilized cell concentration and total cell concentration (4.19 and 5.09 g/l, respectively) was obtained from 2 mm bead diameter system due to the highest surface area for mass transfer. Although, the immobilized cell concentration and total cell concentration of 6 mm bead diameter system (3.50 and 4.23 g/l, respectively) was lower than the other size, the

ethanol concentration and production yield were quite comparable to those of other systems.

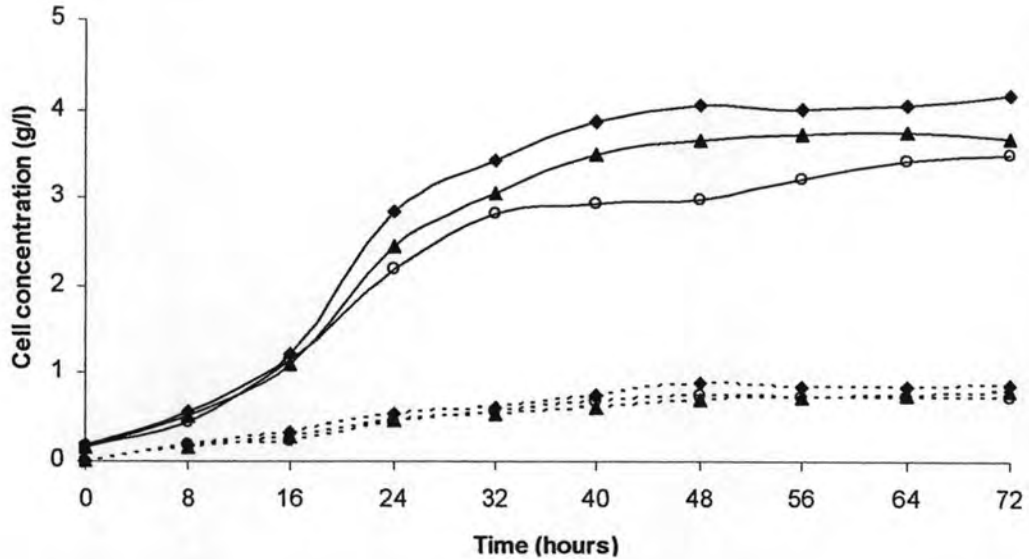


**Figure 4.14** Effect of bead diameter on immobilized cell concentration and free cell concentration of AEC carrier; Immobilized cell concentration (solid lines) and Free cell concentration (dash lines);  $\blacklozenge$ ,  $\varnothing$  2 mm;  $\blacktriangle$ ,  $\varnothing$  4 mm and  $\circ$ ,  $\varnothing$  6 mm

### 4.3 Effect of alginate concentration

Entrapment methods were based on the inclusion of cells within a rigid network to prevent the cells from diffusing into the surrounding medium, while still allowing mass transfer of nutrients and metabolites. Cell growth in the porous matrix depends upon diffusion limitations imposed by the porosity of the material and later by the impact of accumulating biomass. [12]

As the importance of diffusion limitation, the effect of Na-alginate concentration was investigated in this study. Yeast cells were immobilized in 6 mm bead diameter of the AEC carrier with 5% (w/v of alginate) of  $\text{Al}_2\text{O}_3$  that was prepared from different concentration of Na-alginate (1.5%, 2.0%, 2.5% and 3.0% w/v). The fermentation was performed in batch shaking flask with initial sugar concentration of 218 g/l. The results of the fermentation are summarized in Table 4.4. The pattern of ethanol production and

sugar consumption during the fermentation process at various Na-alginate concentrations were shown in Figure 4.15.

**Table 4.4** Yield and end products of batch ethanol fermentation for 72 hours using the cultures of AEC carrier with Na-alginate concentration of 1.5%, 2.0%, 2.5% and 3.0%

Na-alginate conc. (%)	Ethanol concentration (g/l)	Residual sugar concentration (g/l)	Free cell (g/l)	Immobilized cell (g/l)	$Y_I$ (%)	$Y_{P/S}$ (%)
1.5	73.29	44.88	0.90	3.55	79.76	42.44
2.0	75.65	41.95	0.78	3.68	82.50	43.08
2.5	77.76	41.70	0.73	3.72	83.50	44.21
3.0	71.56	49.58	0.67	3.42	83.62	42.60

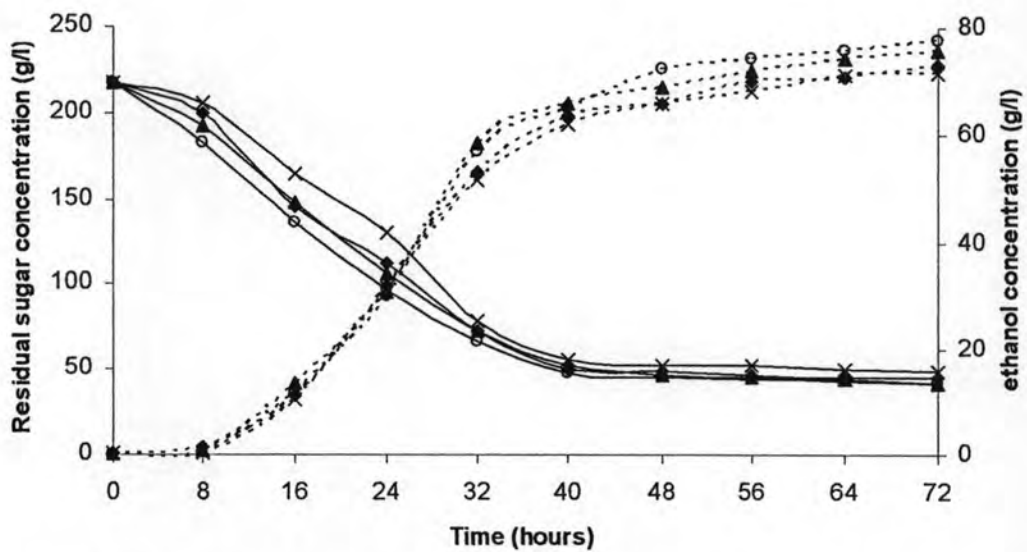


**Figure 4.15** Effect of Na-alginate concentration on residual sugar concentration and ethanol concentration of AEC carrier; Residual sugar concentration (solid lines) and Ethanol concentration (dash lines);  $\blacklozenge$ , 1.5 %;  $\blacktriangle$ , 2.0 %;  $\circ$ , 2.5 % and  $\times$ , 3.0 %

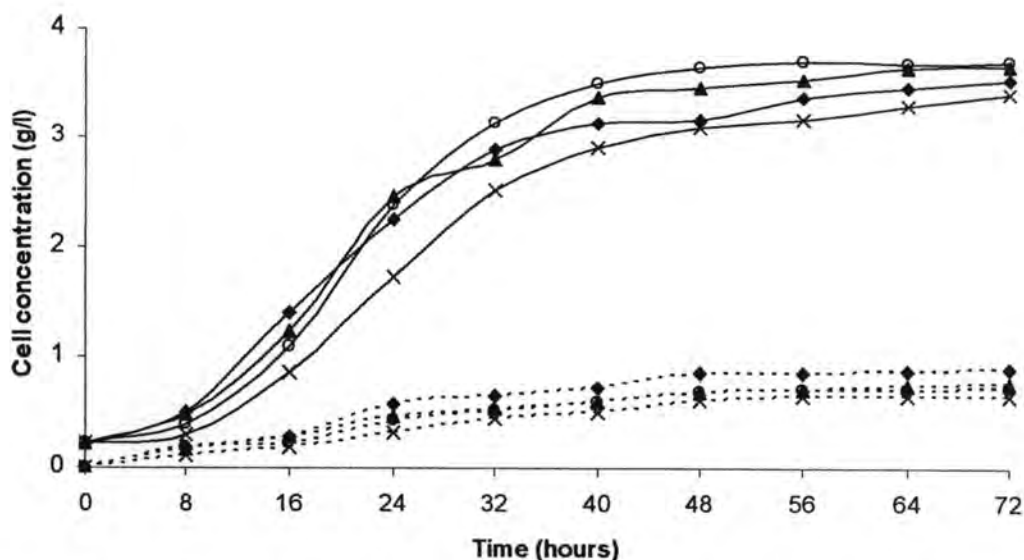


**Figure 4.16** Effect of Na-alginate concentration on immobilized cell concentration and free cell concentration of AEC carrier; Immobilized cell concentration (solid lines) and Free cell concentration (dash lines);  $\blacklozenge$ , 1.5 %;  $\blacktriangle$ , 2.0 %;  $\circ$ , 2.5 % and  $\times$ , 3.0 %

The yeast cells in the 2.5% Na-alginate concentration produced ethanol (77.76 g/l) and utilized sugar ( $Y_{P/S}$  44.21%) better compared to other Na-alginate concentrations. Although the ethanol production and yield value obtained from 2.0% Na-alginate (75.67 g/l and 43.08%) and 2.5% Na-alginate (77.76 g/l and 44.21%) were comparable, the system of 2.0% Na-alginate bead was produced more cells leakage. With the higher Na-alginate concentration, the greater mechanical strength of the bead was obtained. As shown in Figure 4.16, the cell leakages of 1.5% Na-alginate system were the highest. The low Na-alginate concentration created very soft beads which were easily broken because of their low mechanical strength. For the operation in packed bed reactor, it was suggested that the alginate bead with Na-alginate concentration lower than 2.5% Na-alginate concentration could cause the compaction of the gel bead resulting in the bead disintegration and maldistribution of fluid flow. For 3.0% Na-alginate concentration, the ethanol production (71.56 g/l) was decreased probably due to the lower mass diffusion through the dense beads. Although the immobilized yield of 3.0% Na-alginate concentration system was the highest (83.62%), the total cell concentration was the

lowest (4.09 g/l). It could be indicated that the rigid matrix formed lower cell leakage caused by higher mechanical strength and lower cell growth. However, from the limitation of internal diffusion, yeast cells did not get enough nutrients for growth and metabolism of cells. This demonstrated that the diffusion limitation did affect to the ethanol production when the Na-alginate concentration was increased more than 2.5% (w/v).

The result revealed that the suitable Na-alginate concentration for application in ethanol fermentation was 2.5%. In comparison with the previous work, Göksungur et al. (2001) studied the effect of Na-alginate concentration in range of 1.0 - 3.5% (w/v) in packed bed reactor and reported that 2.0% Na-alginate concentration was suitable for ethanol production [26]. Najafpour et al. (2004) tested the hardness and rigidity of alginate beads with the Na-alginate concentration of 1.5 - 6.0% (w/v) [20]. The finding of Najafpour et al. was similar with Göksungur et al. that the highest ethanol production was achieved from 2.0% Na-alginate concentration. However, the developed AEC carrier from this work could create the porous structure within the gel matrix, therefore, the optimal alginate concentration for construction of the AEC bead was relatively higher than that of the conventional alginate bead (EC). Moreover, the use of higher Na-alginate concentration (2.5%) could increase the mechanical strength of the bead which is preferable to the use in packed bed reactor. Since, the addition of  $\text{Al}_2\text{O}_3$  into the gel bead has influence on cell activities, the matrix structure and mechanical strength of the developed bead, therefore, the optimal  $\text{Al}_2\text{O}_3$  concentration for the bead construction was investigated in the further study.

#### **4.4 Effect of alumina ( $\text{Al}_2\text{O}_3$ ) concentration**

With the binding of cell and  $\text{Al}_2\text{O}_3$  particle, the network of  $\text{Al}_2\text{O}_3$  – cell could construct inside the bead. The previous result showed that it could support cell growth and increase porosity inside the bead. In this study, the effect of  $\text{Al}_2\text{O}_3$  concentration on



the cell activities was examined by using 6 mm bead diameter size and 2.5% (w/v) of Na-alginate which was found as the most favorable condition for ethanol production.

**Table 4.5** Yield and end products of batch ethanol fermentation for 72 hours using the cultures of AEC carrier with  $\text{Al}_2\text{O}_3$  concentration of 3.3%, 5.0%, 6.7% and 8.3% (w/v of alginate)

$\text{Al}_2\text{O}_3$ conc. (%)	Ethanol concentration (g/l)	Residual sugar concentration (g/l)	Free cell (g/l)	Immobilized cell (g/l)	$Y_I$ (%)	$Y_{P/S}$ (%)
3.3	72.31	33.91	0.72	3.30	82.08	41.40
5.0	75.03	36.61	0.75	3.48	82.28	43.64
6.7	74.73	35.51	0.76	3.40	81.82	43.19
8.3	67.69	40.07	0.89	3.10	77.75	40.18

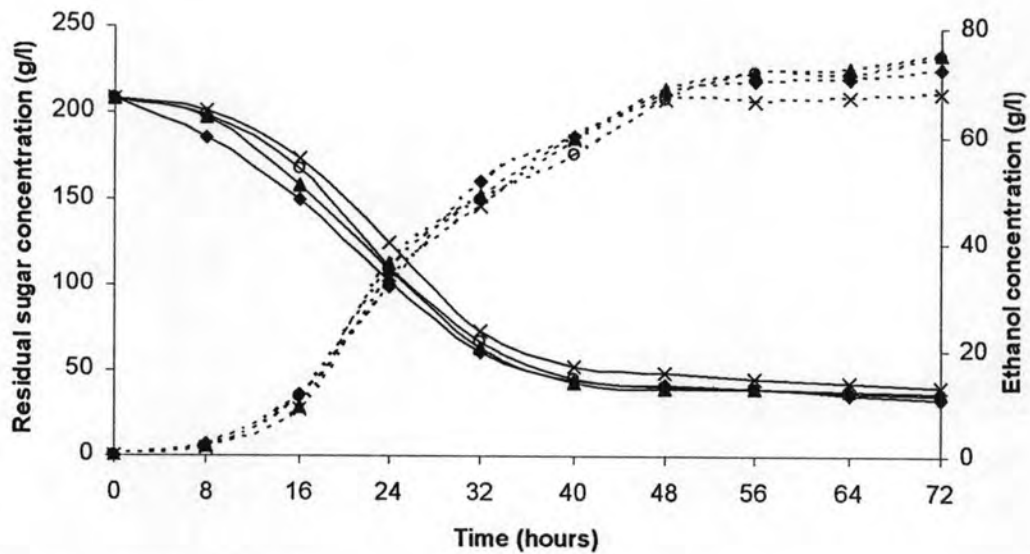


**Figure 4.17** Effect of  $\text{Al}_2\text{O}_3$  concentration on residual sugar concentration and ethanol concentration of AEC carrier; Residual sugar concentration (solid lines) and Ethanol concentration (dash lines);  $\blacklozenge$ , 3.3 %;  $\blacktriangle$ , 5.0 %;  $\circ$ , 6.7 % and  $\times$ , 8.3 %

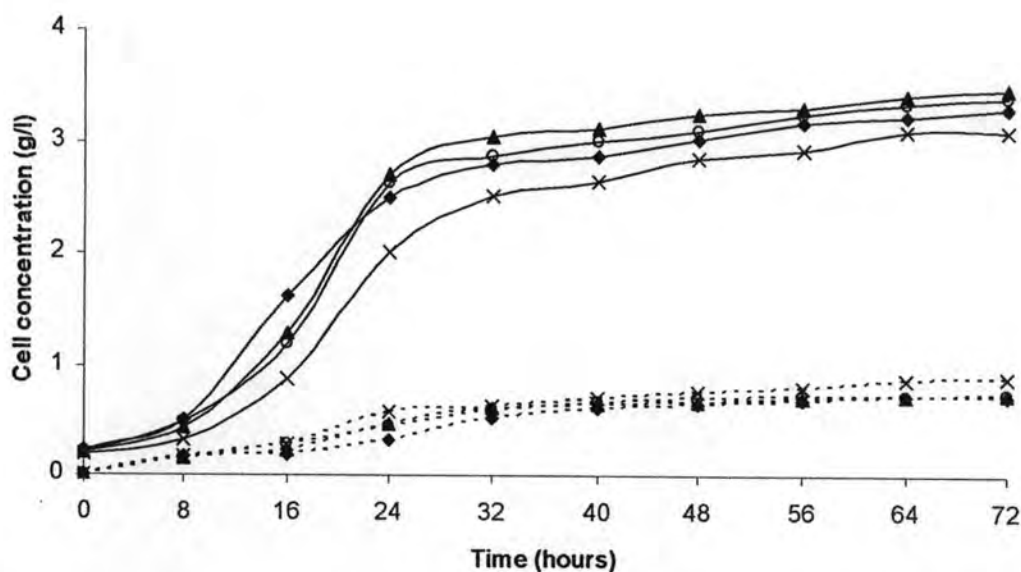


**Figure 4.18** Effect of Al<sub>2</sub>O<sub>3</sub> concentration on immobilized cell concentration and free cell concentration of AEC carrier; Immobilized cell concentration (solid lines) and Free cell concentration (dash lines); ◆, 3.3 %; ▲, 5.0 %; ○, 6.7 % and ×, 8.3 %

The effect of various Al<sub>2</sub>O<sub>3</sub> concentrations (3.3%, 5.0%, 6.7% and 8.3% (w/v of alginate)) on the ethanol production of immobilized *S.cerevisiae* M30 was illustrated in Figure 4.17. The fermentation was performed in batch shaking flask with initial sugar concentration of 209 g/l. The end products of the fermentation are summarized in Table 4.5. The highest ethanol production (75.03 g/l) was obtained from the system applied with 5.0% of Al<sub>2</sub>O<sub>3</sub>. Overall, the final ethanol concentration, residual sugar concentration, free cell concentration and immobilized cell concentration in the system of 5.0% (75.03, 36.61, 0.75 and 3.48 g/l, respectively) and 6.7% (74.73, 35.51, 0.76 and 3.4 g/l, respectively) of Al<sub>2</sub>O<sub>3</sub> were comparable. Whereas, the application of Al<sub>2</sub>O<sub>3</sub> at 3.3% and 8.3% resulted in lower cell and ethanol production.

In the system of the carrier with the low Al<sub>2</sub>O<sub>3</sub> addition at 3.3% (w/v of alginate), the ethanol production and sugar consumption was relatively lower, however, the immobilization yield was similar to that at 5.0 - 6.7% (w/v of alginate) Al<sub>2</sub>O<sub>3</sub>. It was observed that the amount of free cells increased while the immobilization yields decreased with the increase of Al<sub>2</sub>O<sub>3</sub> content in the carriers which was shown in Table 4.5

and Figure 4.18. It might be explained that the addition of  $\text{Al}_2\text{O}_3$  in the carrier created the more porous structure and caused the less denser gel structure. As a result, with the high  $\text{Al}_2\text{O}_3$  addition at 8.3% (w/v of alginate) the gel structure of the carrier become loose and was easy breakable. It was also observed that with the optimal range of  $\text{Al}_2\text{O}_3$  addition, 5.0 – 6.7% (w/v of alginate), the addition of  $\text{Al}_2\text{O}_3$  supported cell growth and ethanol formation. However, at high  $\text{Al}_2\text{O}_3$  content at 8.3% (w/v of alginate), the ethanol production and immobilized cells decreased. Since yeast were bound with  $\text{Al}_2\text{O}_3$  by electrostatic force, the excess of  $\text{Al}_2\text{O}_3$  was possible created high positive charge density in immobilized cell system that might be considered negative interfering in the activities of the cell.

The result demonstrated that the content of  $\text{Al}_2\text{O}_3$  in the AEC carrier had influence on cell growth and product formation. At 5.0% of  $\text{Al}_2\text{O}_3$  concentration gave the maximum ethanol production compared with the others.

Therefore, for the development of AEC carrier for ethanol fermentation in packed bed column, the selected condition was at 2.5% (w/v) of Na-alginate and 5.0% (w/v of alginate) of  $\text{Al}_2\text{O}_3$  with bead diameter of 6 mm. However, to be easy to handle in the large scale, the next experiment attempt was to modify the shape of the AEC carrier which was convenient for the scale up.

#### **4.5 Modification of AEC carrier shape**

From the restriction of the sphere shape ( $\text{Ø}$  6 mm) immobilized cell preparation, this work effort to modify the AEC carrier shape for the scale up in 1 L packed bed reactor. The square shape ( $20 \times 20 \times 4 \text{ mm}^3$ ) immobilized cell carrier were examined in this study. It was prepared by pouring the Na-alginate-  $\text{Al}_2\text{O}_3$ -cell solution to the tray and then cross linking by 0.12M  $\text{CaCl}_2$  solution. After that it was soaked in  $\text{CaCl}_2$  solution for 30 minutes, it was cut in square shape of  $20 \times 20 \times 4 \text{ mm}^3$  by scissor. A piece of square shape (1.25 ml) had more volume than sphere shape (0.375 ml) and easier for prepared in

large amount. Therefore, the competence of square shape carrier on ethanol production was observed in shaking flask and 1 L packed bed reactor.

**Table 4.6** Yield and end products of batch ethanol fermentation for 72 hours using the cultures of AEC carrier with 2.5% of Na-alginate and 5.0% of Al<sub>2</sub>O<sub>3</sub> in square and sphere shape in shaking flask.

<b>Shape</b>	<b>Ethanol concentration (g/l)</b>	<b>Residual sugar concentration (g/l)</b>	<b>Free cell (g/l)</b>	<b>Immobilized cell (g/l)</b>	<b>Y<sub>I</sub> (%)</b>	<b>Y<sub>P/S</sub> (%)</b>
square	89.83	26.84	0.86	3.56	80.47	44.68
sphere	90.92	25.84	0.78	3.72	82.70	45.45

Yeast cells were immobilized in sphere shape (Ø 6 mm) and square shape (20 x 20 x 4 mm<sup>3</sup>) of the AEC carrier which was prepared from 2.5% of Na-alginate and 5.0% of Al<sub>2</sub>O<sub>3</sub>. The fermentation was performed in batch shaking flask with initial sugar concentration of 227 g/l. The results of the fermentation are summarized in Table 4.6. The final ethanol concentration of square shape and sphere shape system were 89.83 and 90.92 g/l, respectively and the final sugar concentration were 26.84 and 25.84 g/l, respectively (Y<sub>P/S</sub> 44.68% and 45.45%, respectively). The ethanol formation and sugar consumption trends of square and sphere shape system were comparable as shown in Figure 4.19. Although, at the beginning, the ethanol concentration of square shape system was slightly lower than that of sphere shape system, the final ethanol concentration of square shape system increased until it reached to the similar level of the sphere shape system. This result could be concluded that at the end of fermentation the ethanol production of square shape system was not significant different from that of the sphere shape system.

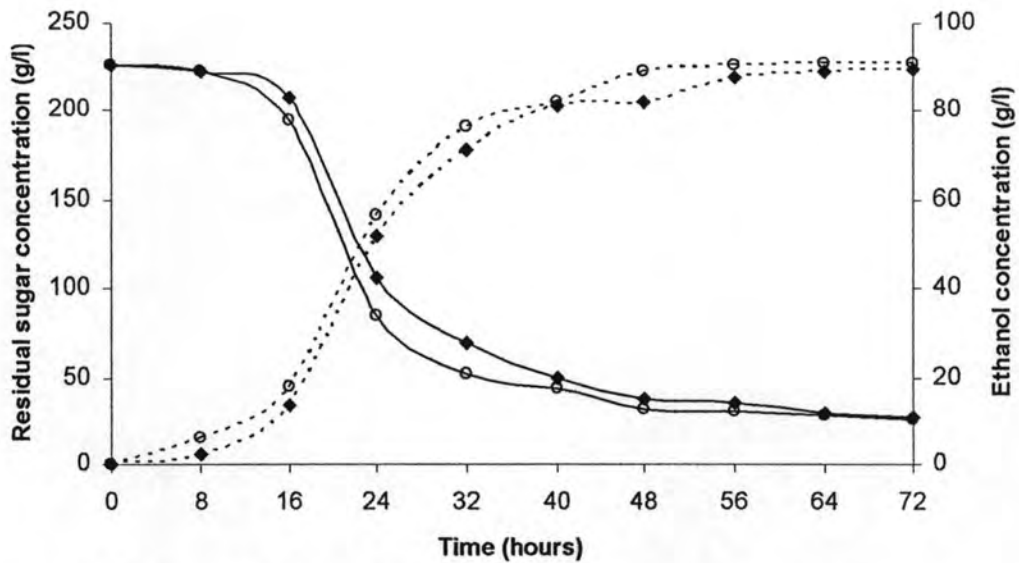


**Figure 4.19** Effect of AEC carrier expansions on residual sugar concentration and ethanol concentration of AEC carrier; Residual sugar concentration (solid lines) and Ethanol concentration (dash lines); ◆, square shape and ○, sphere shape

For the cell information, free cells were harvested every 8 hours while immobilized cells were harvested at 0, 32, 64 and 72 hours due to the large volume per piece of square shape was sampling that would reduce amount of cell in the fermentation system. As shown in Figure 4.20, the immobilized cell concentration of the sphere shape system was higher than the square shape systems and the leakage cell was slightly lower. However, at the end of the fermentation the total cell concentration of the sphere shape (4.50 g/l) and the square shape (4.42 g/l) system were comparable. This was discussed that the sphere shape carrier could contact with substrate better than the square shape because of fluid motion around the sphere shape was more distribution. Although the ethanol production and immobilized cell generation of the square shape system slightly delayed from the sphere shape system, the preparation of square shape was easier and more convenient for the large scale production.

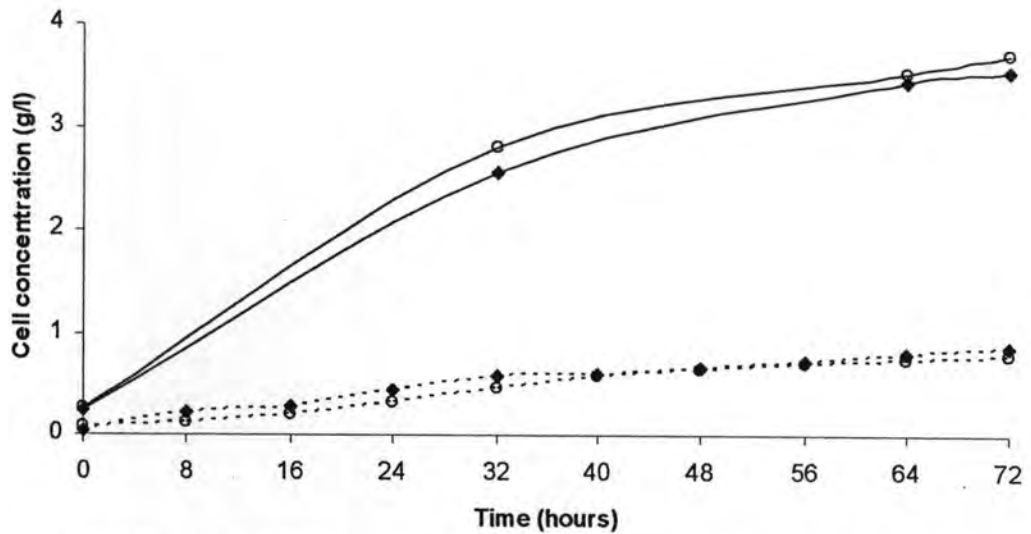


**Figure 4.20** Effect of AEC carrier expansions on residual sugar concentration and ethanol concentration of AEC carrier; Immobilized cell concentration (solid lines) and Free cell concentration (dash lines); ◆, square shape and ○, sphere shape

#### 4.6 Mechanical properties testing

Since the cell carrier should have good mechanical property to be able to retain its shape under pressure changes or shearing force, the mechanical properties in term of tensile strength and percentage elongation at break of the AEC carrier at the concentration of 2.5% Na-alginate and 5.0%  $\text{Al}_2\text{O}_3$  was investigated and compared to those of the EC carrier at the same Na-alginate concentration. The sample in dimension of  $10 \times 100 \times 4 \text{ mm}^3$  of AEC and EC carrier was prepared by pouring of the immobilized cell solution to the tray and then cross linking with 0.12M  $\text{CaCl}_2$  solution. Each piece was cut by scissor while it was soaked in 0.12M  $\text{CaCl}_2$  solution.

Tensile strength measures material strength, whereas percentage elongation at break is an indicator of toughness and stretch-ability prior to breakage. These parameters dictate the end-use handling properties and mechanical performance of the material [36]. Mechanical properties of AEC and EC carrier were summarized in Figure 4.21 and 4.22. Tensile strength and percentage elongation at break values of AEC carrier (0.24 MPa and 80.8%, respectively) were significantly higher than those of EC carrier (0.17 MPa and

57.1%, respectively). The greater strength and flexibility of AEC carrier might be caused by the presence of  $\text{Al}_2\text{O}_3$  particle that constructed the cell -  $\text{Al}_2\text{O}_3$  network inside the gel and help to support, link or hold the molecule together. It exhibited that the structure of AEC carrier had better mechanical property than that of the EC carrier.

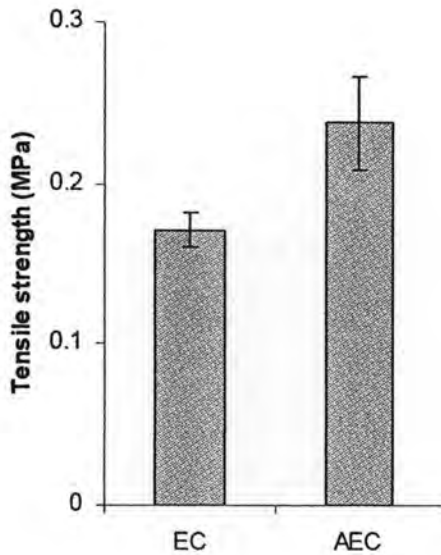


**Figure 4.21** Tensile strength of AEC and EC carriers

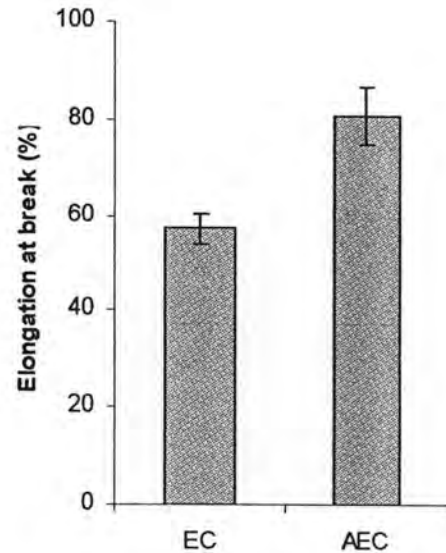


**Figure 4.22** Elongation at break of AEC and EC carriers

#### 4.7 Pore characteristics testing

Surface area and porosity are important characteristics, capable of affecting the quality and utility of many materials [37]. Likewise, knowledge of porosity and surface area are frequently important keys in understanding the structure, formation and potential applications of the cell carrier. Thus, the structure parameters such as pore diameter, surface area, porosity, and pore volume of the AEC carrier at the concentration of 2.5% Na-alginate and 5.0%  $\text{Al}_2\text{O}_3$  was investigated and compared to those of the EC carrier at the same Na-alginate concentration. The sample of AEC and EC carrier was prepared in the spherical shape at 6 mm bead diameter size. The information on the porous structure

was evaluated through the nitrogen adsorption isotherms using BET (Brunauer-Emmett-Teller) and BJH (Barrett-Joiner-Halenda) methods (Micrometrics-ASAP2000).

**Table 4.7** Pore characteristics of EC carrier, AEC carrier and Al<sub>2</sub>O<sub>3</sub> powder

System	BET Specific surface area (m <sup>2</sup> /g)	Pore diameter (nm)	Pore volume (cc/g)	Porosity (%)
EC	60.24	14.20	0.27	24.62
AEC	119.08	15.33	0.49	41.81
Al <sub>2</sub> O <sub>3</sub> powder	0.72	16.03	0.0036	4.31

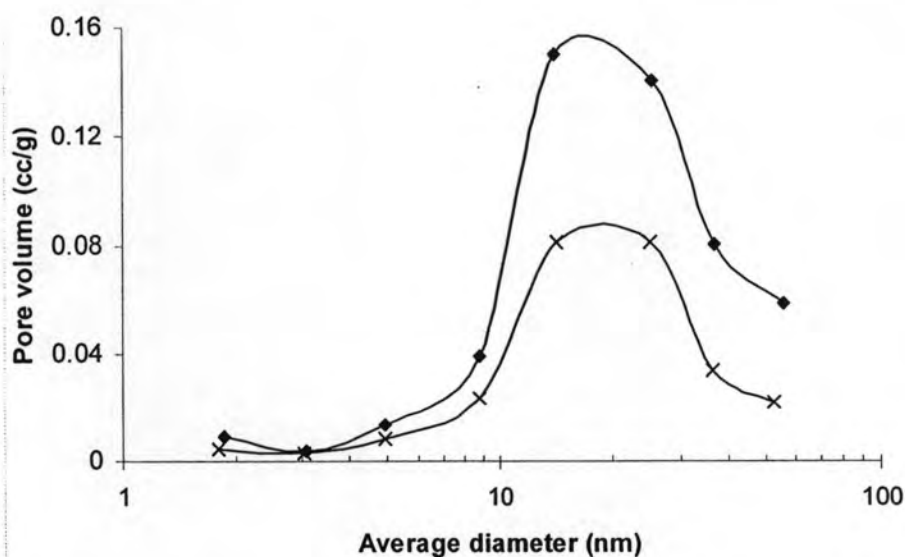


**Figure 4.23** Pore volume versus average pore diameter of the carriers; ◆, AEC carrier and ×, EC carrier

Pore characteristics of EC carrier, AEC carrier and Al<sub>2</sub>O<sub>3</sub> powder were summarized in Table 4.7. It was shown that BET specific surface area, pore diameter, pore volume and porosity of AEC carrier were significantly higher than those of EC carrier. According to the comparison of the BET specific surface area of EC carrier, AEC carrier and Al<sub>2</sub>O<sub>3</sub> powder revealed that the higher BET specific surface area of AEC



carrier should cause by the formation of microporous structure from the network of  $\text{Al}_2\text{O}_3$ -cell inside the carrier; not from the surface area of  $\text{Al}_2\text{O}_3$  powder. Figure 4.23 showed the comparison of pore distribution and pore volume between the AEC and EC carriers. The better porosity of AEC carrier could enhance the mass transfer rate of substrate and product across the carrier matrix. It revealed that the structure of AEC carrier had better pore characteristics than that of the EC carrier.

#### 4.8 Continuous ethanol fermentation in packed bed reactor

Continuous fermentation in packed bed reactor offers important advantages, such as higher conversion rates, faster overall fermentation rates, improved product consistency, reduced product losses and environmental advantages. An important aspect of continuous fermentation is the high volumetric efficiency, which is usually obtained by increased yeast cell concentrations in the reactor compared to traditional batch systems. The high cell densities are achieved by using cell immobilization technique which, in combination with high flow rates, leads to short residence times [3]. These benefits are the driving force for this research effort aimed at studying and implementing in continuous process. Ethanol fermentation with immobilized cells was generally performed in packed bed reactor due to simple design and operational control [24]. The current work was carried out in a packed-bed bioreactor (PBR).

PBR containing *S.cerevisiae* M30 immobilized in AEC ( $20 \times 20 \times 4 \text{ mm}^3$ , 2.5% of Na-alginate and 5.0% of  $\text{Al}_2\text{O}_3$ ) carrier was used for continuous ethanol fermentation. Under the following conditions: working volume 0.60 L, temperature  $32 \pm 1^\circ\text{C}$ , initial sugar concentration about 223 g/l, initial pH 5. The dilution rate was tested which was varied from 0.09, 0.16, 0.22 to  $0.28 \text{ h}^{-1}$ , it was corresponding to a hydraulic retention time (HRT) from 11.11, 6.25, 4.55 to 3.57 h, respectively. Prior to inoculation and start up of the fermentation, the column was sterilized by circulation of 70% v/v ethanol for 1 hour and then was kept under UV light overnight. The immobilized cells in AEC carrier was cultivated with initial sugar concentration about 223 g/l in shaking flask at 150 rpm,  $33^\circ\text{C}$

for 24 hour that to increase the cells concentration in AEC carrier before the carries were aseptically transferred to the sterilized column. The carrier volume was about 40% (v/v) of the pack bed reactor volume of 1 L. A start-up procedure was required in order to establish a steady state phase. Initially, the fermentation was started by feeding of the prepared medium of sugar cane molasses (223 g/l), through the inlet (1<sup>st</sup> sampling port, Figure 3.2) at the bottom of the column at the dilution rate of 0.09 h<sup>-1</sup>. The dilution rate was changed after 4 days of 0.09 h<sup>-1</sup> dilution rate and after 3 days of 0.16, 0.22 and 0.28 h<sup>-1</sup> dilution rates. The samples were harvested every 8 hours from the 5<sup>th</sup> sampling port of the column (Figure 3.2 and Figure 4.24). After the operation with the dilution rate of 0.28 h<sup>-1</sup> for 3 days, the dilution rate was rolled back to the start dilution rate (0.09 h<sup>-1</sup>) for stability checking of the cell activities for 17 days, in which, the samples were harvested every 24 hours.

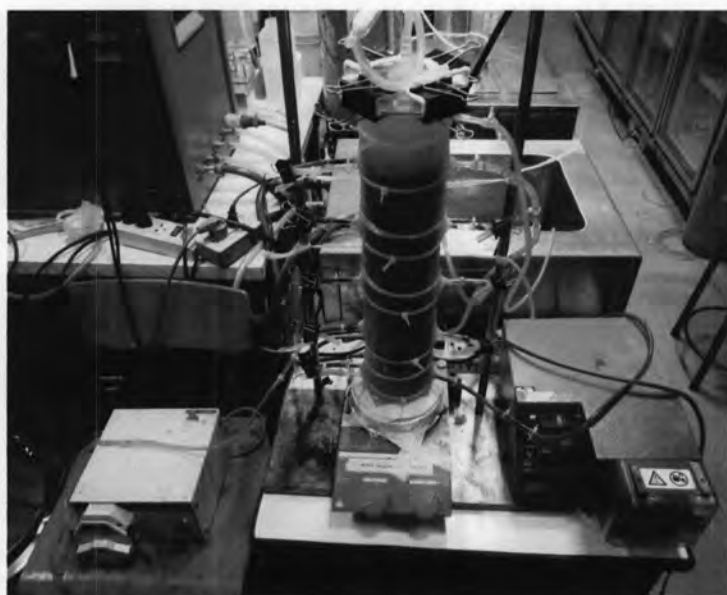


**Figure 4.24** Picture of PBR

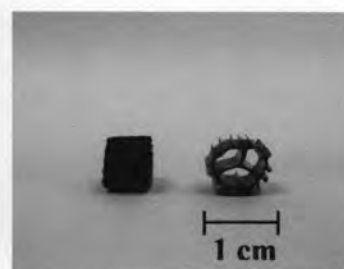


**Figure 4.25** The porous plastic material (PVA)

From the preliminary test, the compaction of gel carrier was found after 3 days of the operation, which cause the maldistribution flow of substrate and product in the bed (data not show). So, this problem was fixed by divided the bed into 9 stage by the tray packed with porous plastic (PVA) material (Figure 4.25) for improved flow distribution. Therefore, the reactor became a 9 multistage PBR. A magnetic bar was place in the bottom of the reactor for well mixing of substrate. Moreover, at the end of each dilution rate and every 3 days in the stability test period, the recycle process was used to disperse the accumulated CO<sub>2</sub> in the beds. The recycle process was done by connected the sterilized silicone tube from the outlet tube at the 5<sup>th</sup> sampling port into the inlet tube at the 1<sup>st</sup> sampling port on both sides of the column for the circulation of the fluid for 45 minutes (about circulate 10 cycles).

**Table 4.8** Effect of dilution rate on continuous ethanol production and ethanol productivity, average at steady state

<b>Dilution rate (h<sup>-1</sup>)</b>	<b>Ethanol concentration (g/l)</b>	<b>Residual sugar concentration (g/l)</b>	<b>Y<sub>P/S</sub> (%)</b>	<b>Productivity (g/l · h)</b>
0.09	86.58 (± 1.33)	20.40 (± 1.71)	42.73	7.79 (± 0.19)
0.16	68.49 (± 1.37)	64.58 (± 2.15)	43.23	10.96 (± 0.22)
0.22	53.35 (± 2.00)	102.53 (± 3.50)	44.28	11.74 (± 0.44)
0.28	44.09 (± 1.77)	124.89 (± 4.26)	44.93	12.34 (± 0.50)

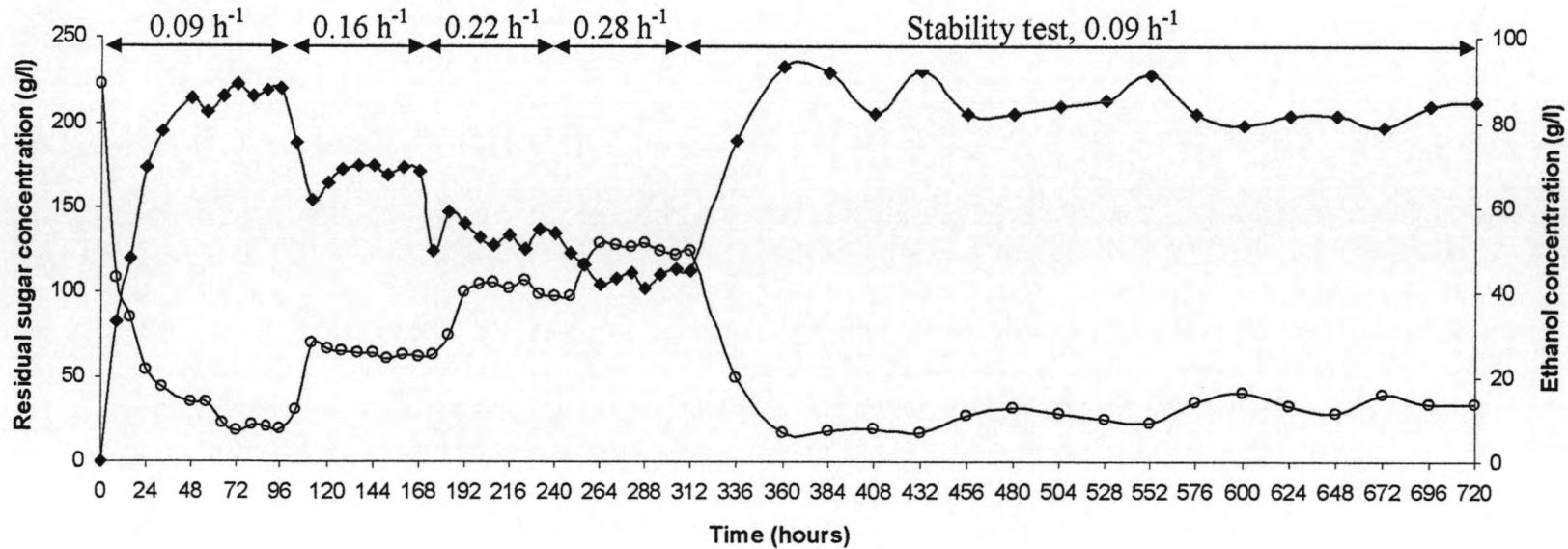


Figure 4.26 Continuous fermentation in a PBR at the dilution rate of 0.09, 0.16, 0.22 and 0.28 h<sup>-1</sup>;  
 ○, Residual sugar concentration and ◆, Ethanol concentration

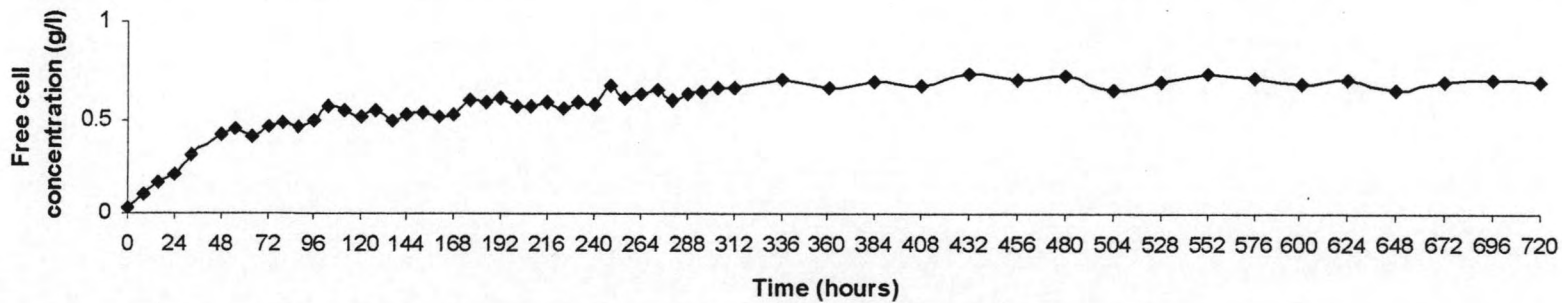


Figure 4.27 Continuous fermentation on free cell (effluent) concentration in a PBR

The ethanol production and the sugar consumption at various dilution rates were shown in Figure 4.26. Ethanol production, sugar consumption and productivity after the steady state of various dilution rates were shown in Table 4.8. As expected, the highest steady-state ethanol concentration ( $86.58 \pm 1.33$  g/l) and the lowest residual sugar concentration ( $20.40 \pm 1.71$  g/l) were obtained at the lowest dilution rate ( $0.09$  h<sup>-1</sup>). The obtained steady state concentrations at  $0.09$  h<sup>-1</sup> dilution rate were comparable to the final concentration obtained in the previous batch operation. This result demonstrated that the AEC carrier and the operating condition were suitable and reliable for continuous ethanol fermentation by *S.cerevisiae* M30. As the dilution rates were increased to  $0.16$ ,  $0.22$  and  $0.28$  h<sup>-1</sup>, after steady state, the ethanol concentrations were at  $68.49 \pm 1.37$ ,  $53.35 \pm 2.00$  and  $44.09 \pm 1.77$  g/l, respectively and the residual sugar concentrations were at  $64.58 \pm 2.15$ ,  $102.53 \pm 3.50$  and  $124.89 \pm 4.26$  g/l, respectively. This result indicated that the outlet ethanol concentration decreased when the dilution rate increased due to the decrease of the residence time. Production yields in the operated range of dilution rate ( $0.09 - 0.28$  h<sup>-1</sup>) varied only slightly from  $0.42$  to  $0.45$ .

The effect of dilution rate on ethanol productivity was illustrated in Figure 4.28, it was indicated that the ethanol productivity increased as the dilution rate was increased. The productivity increased from  $7.79$  g/l · h at the lowest dilution rate ( $0.09$  h<sup>-1</sup>) to  $12.34$  g/l · h at a dilution rate of  $0.28$  h<sup>-1</sup>. In term of ethanol productivity with the operation in PBR at the dilution rate of  $0.09$  h<sup>-1</sup>, the productivity was approximately 6 times greater than that of the batch operation ( $1.40$  g/l · h).

To confirm the consistency of performance and stability of yeast cells, the system was operated for 30 days and the yeast cells in the reactor were found still effective and stable within the AEC carrier through the entire experiment. This could be supported from the results of the ethanol concentration and the sugar consumption when the dilution rate was turned back to  $0.09$  h<sup>-1</sup> (Figure 4.26 and 4.29). In the initial period of the operation at  $0.09$  h<sup>-1</sup> dilution rate, the steady state ethanol concentration was at  $86.58 \pm 1.33$  g/l, which was comparable to that in the end period ( $84.30 \pm 5.00$  g/l). During the stability testing, the cell activity was maintained about 97.36% of its original activity.

This means that the immobilized *S.cerevisiae* M30 in AEC carrier retained their metabolic activity to produce ethanol during 30 days of the operation. It should be noted that in the present study, the operation was stopped after 30 days due to our experimental plan without any occurrence of decay indication in the system.

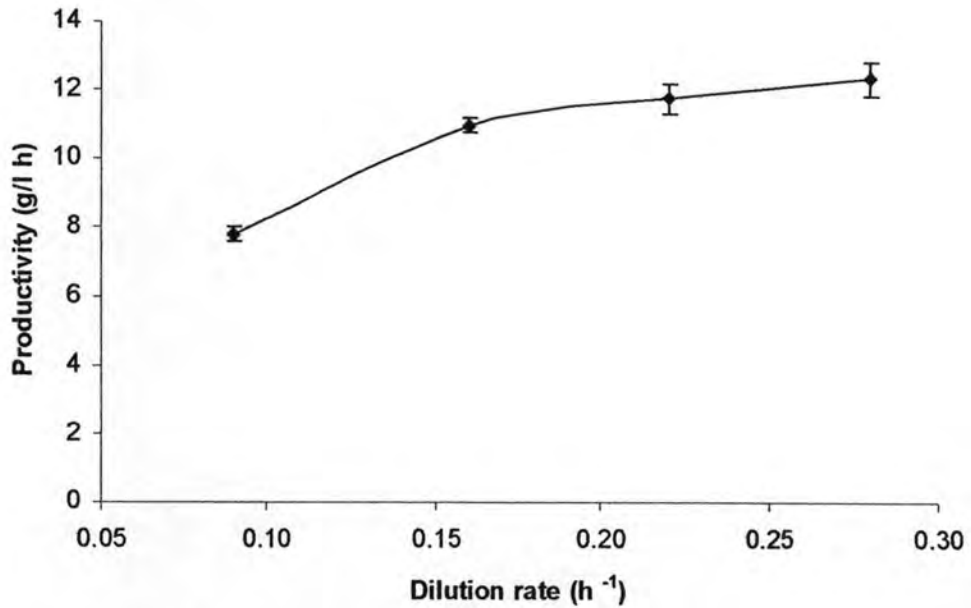


**Figure 4.28** Effect of dilution rate on ethanol productivity

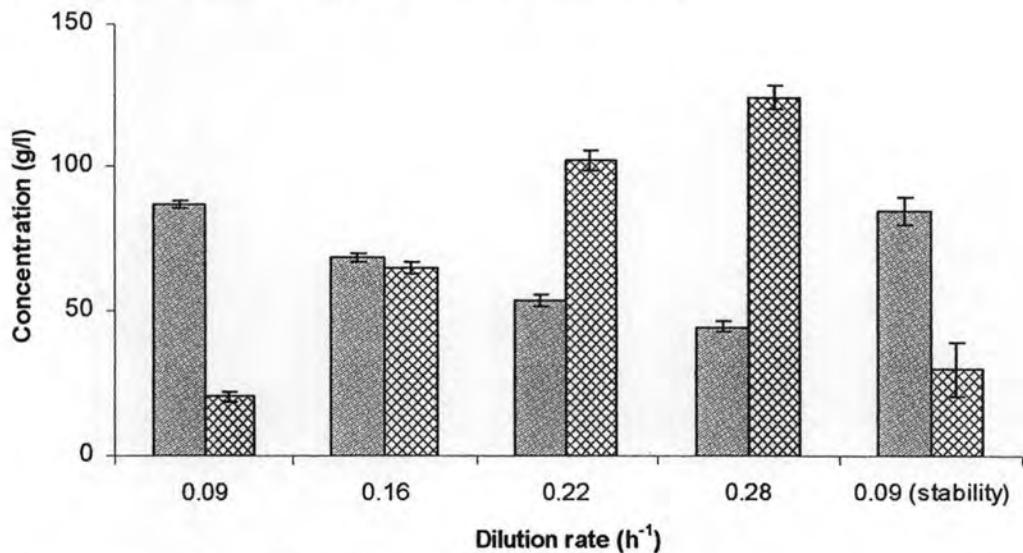


**Figure 4.29** Effect of dilution rate on the ethanol and residual sugar concentration;  
 ■, Ethanol concentration and ▨, Residual sugar concentration

**Table 4.9** Yeast cell concentrations in the PBR

Cell system	Cell concentration (g/l)
Immobilized cell – at completed gelation	0.18
Immobilized cell – at the beginning of fermentation	5.34
Immobilized cell – the end of the fermentation	19.25
Free cell – in the reactor at the end of the fermentation	2.92
Free cell – effluent from the reactor	$0.61 \pm 0.08$
Immobilized yield (%)	84.50

Under steady state conditions, the free cell concentration leaving the reactor at the 5<sup>th</sup> sampling port (Figure 4.27) remained nearly constant ( $0.61 \pm 0.08$  g/l), only increased slightly with operation days which was relatively lower than that in the batch fermentation (0.8 g/l). This exhibited that yeast cells were confined by the bed causing only a few of free cell leaving from the reactor. The immobilized cell concentration increased from 5.34 g/l at the start of operation to 19.25 g/l at the end of operation or about 4 folds from the beginning (Table 4.9). This demonstrated that yeast cells could grow and regenerate inside the AEC carrier when operate in the PBR.

To study the behavior of ethanol fermentation at various HRT (hydraulic retention time), at the steady state of each dilution rate, the samples were harvested at 5 ports (1<sup>st</sup> – 5<sup>th</sup>) of the bed (Figure 4.30 and 4.31, Table 4.10). During the HRT from 0 – 11 hours, the ethanol concentration increased and the residual sugar concentration decreased with increasing HRT. At the same HRT, the ethanol concentration increased with the increased dilution rate. It could be explained that at a constant working volume (HRT), the feed flow rate increased with the dilution rate, therefore, the increase of the dilution rate could reduce the external mass transfer resistance or the resistance of the film layer between the immobilized cell matrix and the solution phase. At the lower dilution rate, the external mass transfer resistance was higher, so that it could cause of slower ethanol production rate. Although, the ethanol productivity at high dilution rate was higher, the

effluent ethanol concentration was more dilute due to the shorter of the reaction time at high feed flow rate.

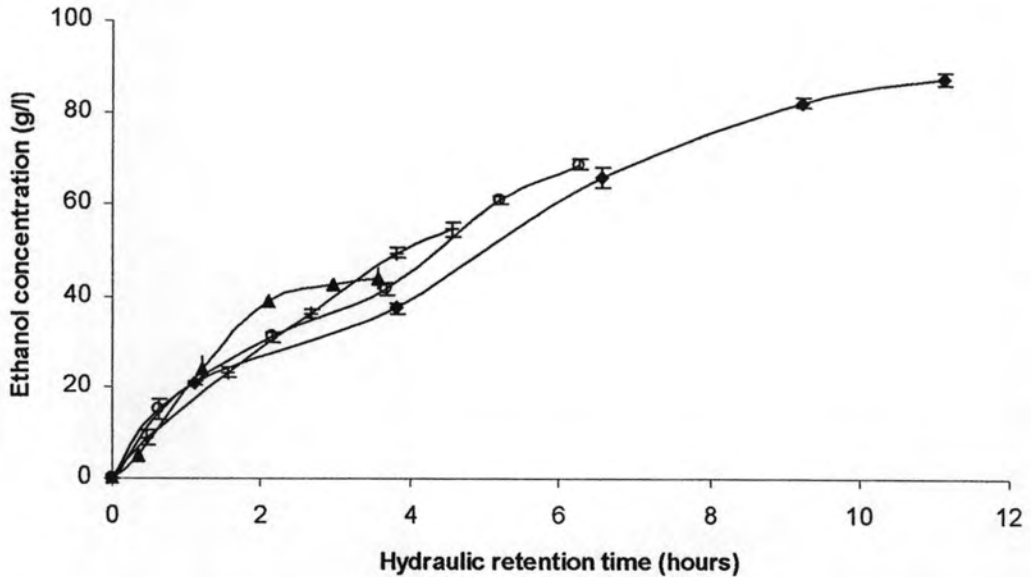


**Figure 4.30** The steady state ethanol concentration at 5 ports of the PBR, average from 3 replications at steady state; ◆, 0.09 h<sup>-1</sup>; ○, 0.16 h<sup>-1</sup>; +, 0.22 h<sup>-1</sup> and ▲, 0.28 h<sup>-1</sup>

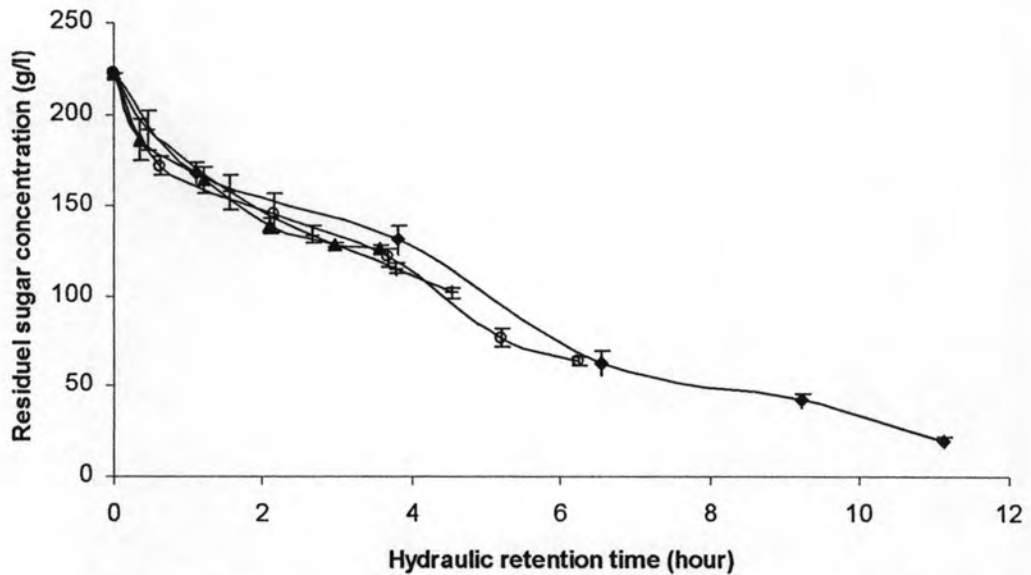


**Figure 4.31** The steady state residual sugar concentration at 5 ports of the PBR, average from 3 replications at steady state; ◆, 0.09 h<sup>-1</sup>; ○, 0.16 h<sup>-1</sup>; +, 0.22 h<sup>-1</sup> and ▲, 0.28 h<sup>-1</sup>



**Table 4.10** The steady state ethanol and residual sugar concentration at 1<sup>st</sup> - 5<sup>th</sup> ports of the PBR, average from 3 replications at steady state

<b>Dilution rate (h<sup>-1</sup>)</b>	<b>Retention time (hours)</b>	<b>Ethanol concentration (g/l)</b>	<b>Residual sugar concentration (g/l)</b>	<b>Productivity (g/l · h)</b>
0.09	0.00	0.00	223.00	
0.09	1.10	20.80 (± 0.63)	169.10 (± 5.65)	18.91
0.09	3.81	37.44 (± 1.24)	130.86 (± 8.78)	9.83
0.09	6.54	66.13 (± 2.31)	62.20 (± 7.28)	10.11
0.09	9.25	82.57 (± 1.31)	41.76 (± 3.98)	8.93
0.09	11.11	87.78 (± 1.56)	19.77 (± 1.78)	7.90
0.16	0.00	0.00	223.00	
0.16	0.62	14.94 (± 2.43)	172.00 (± 5.12)	24.09
0.16	2.15	31.13 (± 1.10)	145.98 (± 10.78)	14.48
0.16	3.68	41.66 (± 1.30)	120.51 (± 5.56)	11.32
0.16	5.21	61.06 (± 1.03)	76.32 (± 5.17)	11.72
0.16	6.25	68.87 (± 1.11)	63.21 (± 1.92)	11.02
0.22	0.00	0.00	223.00	
0.22	0.45	8.81 (± 1.44)	192.21 (± 10.78)	19.57
0.22	1.56	23.22 (± 1.14)	157.91 (± 9.58)	14.88
0.22	2.68	36.25 (± 0.76)	133.64 (± 4.97)	13.53
0.22	3.79	49.55 (± 1.19)	114.76 (± 2.85)	13.07
0.22	4.55	54.70 (± 1.56)	101.55 (± 2.91)	12.02
0.28	0.00	0	223.00	
0.28	0.35	5.08 (± 1.47)	186.60 (± 11.45)	14.51
0.28	1.22	23.92 (± 2.84)	164.85 (± 7.62)	19.60
0.28	2.10	38.79 (± 0.63)	138.95 (± 4.36)	18.47
0.28	2.97	42.76 (± 1.10)	128.28 (± 1.04)	14.40
0.28	3.57	43.76 (± 2.18)	125.06 (± 3.09)	12.26

In commercial ethanol production facilities, productivity was important but was less significant than efficiency of substrate conversion, especially since a major expense of the process was the cost of the fermentable raw material and product separation process. Although our system was primarily designed for efficient substrate conversion to ethanol, the productivities reported in this experiment were competitive with previous reports for a comparable system. Göksungur et al. (2001) studied the production of ethanol from beet molasses by Ca-alginate immobilized yeast cells in a PBR and reported that the ethanol concentration and productivity were 46.18 g/l and 10.16 g/l · h, respectively with the initial sugar concentration and dilution rate of 109 g/l and 0.22 h<sup>-1</sup>, respectively [26]. The work of Najafpour et al. (2004) on the ethanol fermentation in immobilized cell reactor resulted in the ethanol productivity of 2.8 g/l · h with the initial sugar concentration and dilution rate of 50 g/l and 0.17 h<sup>-1</sup>, respectively [20]. However, the fermentation efficiencies obtained in different studies were difficult to compare according to the wide diversity of applied conditions during the fermentation process such as yeast strain, reactor volume, raw material and operating condition.

The pictures of the complete gelation were shown in Figure 4.32 and 4.33. The surface of the carrier was not flat since the cross-link process was occurred outside on the surface first and then inside the carrier. The picture of the carrier at the end of fermentation was shown in Figure 4.34. In comparison with the initial carrier, the carrier at the end of fermentation was darker from the soak in fermentation broth, thicker due to the growth of cell and accumulated CO<sub>2</sub> inside the carrier. However, the width and length of the carrier were slightly shorter caused by the shear force effect during the fermentation in shaking flask period (before the PBR operation). As seen in Figure 4.34, the surface of carrier was covered by the mucosal gel that might be the byproduct from cell reaction or the cell sedimentation. This mucosal gel could be affected to cell activity and on external mass transfer into the carrier.

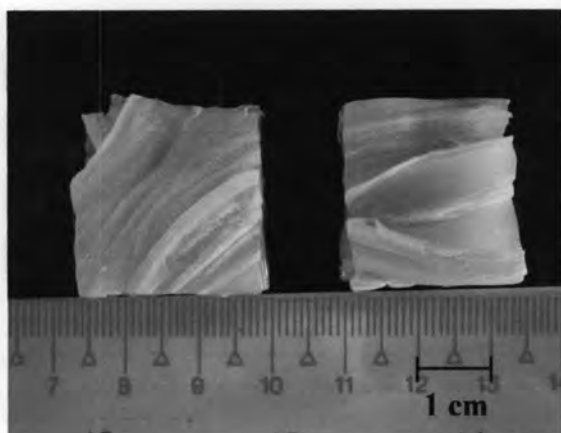


**Figure 4.32** Square shape of AEC carrier at the completed gelation (width and length)

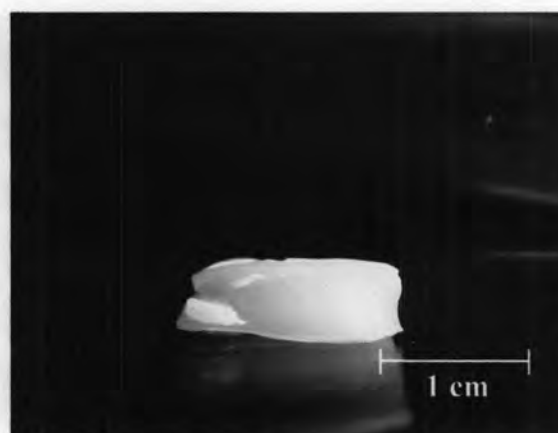


**Figure 4.33** Square shape of AEC carrier at the completed gelation (height)

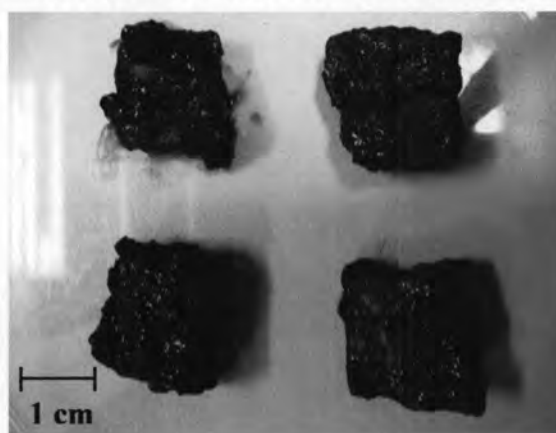


**Figure 4.34** Square shape of AEC carrier at the end of fermentation

SEM investigations were carried out to show the characteristic of the cell immobilization in AEC carrier. The images of the carriers at the completed gelation, the beginning of fermentation and the end of fermentation were investigated. The whole view of the completed gelation (Figure 4.35) demonstrated that the surface was irregular shape but quite smooth. The carrier surface at the end of the fermentation had more opening parts than at the beginning of the fermentation due to the cell growth and formation of  $\text{CO}_2$  inside the carrier (Figure 4.36-4.39). The cross section of carrier from the completed gelation to the end of fermentation (Figure 4.40-4.44) showed that the amount of cell inside the carrier was increased with cultivation time. The cell leakage was observed from free cells in the reactor and free cells in the effluent (Figure 4.45 and 4.46). The

image of free cells in the reactor indicated that a few living cell was still remained in oval shape. No occurrence of contamination by other microorganisms during 30 days of operation. Therefore, the high amount of the yeast cell packing in the reactor together with the effect of ethanol content in the system could dominate the existing of other living and inhibit the growth of contaminating microorganisms.

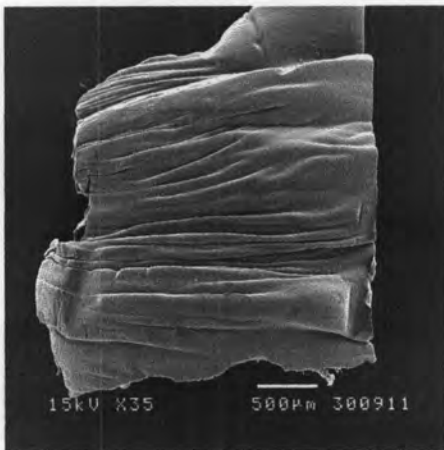


**Figure 4.35** The over view of AEC at the completed gelation (x35)

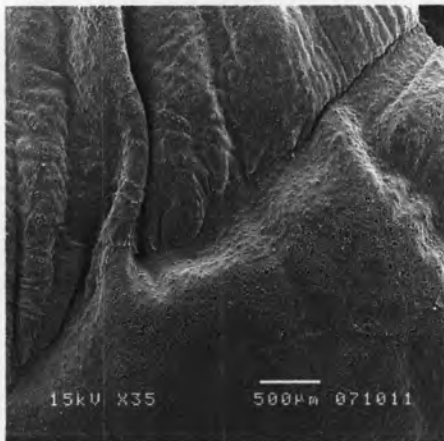


**Figure 4.36** The over view of AEC at the beginning of fermentation (x35)

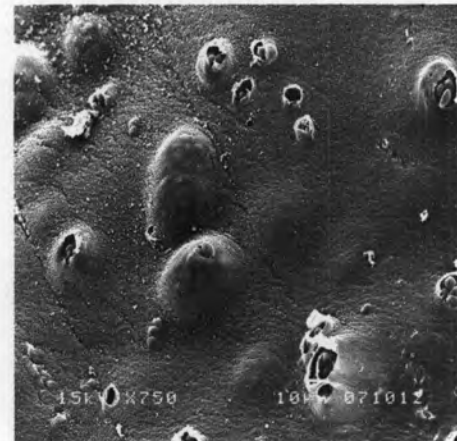


**Figure 4.37** Surface of AEC at the beginning of fermentation (x750)



**Figure 4.38** The over view of AEC at the end of fermentation (x35)



**Figure 4.39** Surface of AEC at the end of fermentation (x750)

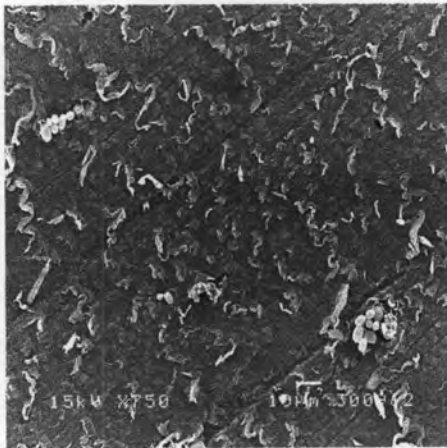


**Figure 4.40** Cross section of AEC at the completed gelation (x750)

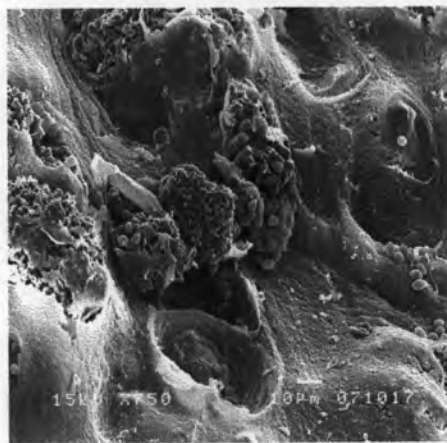


**Figure 4.41** Cross section of AEC at the beginning of fermentation (x750)

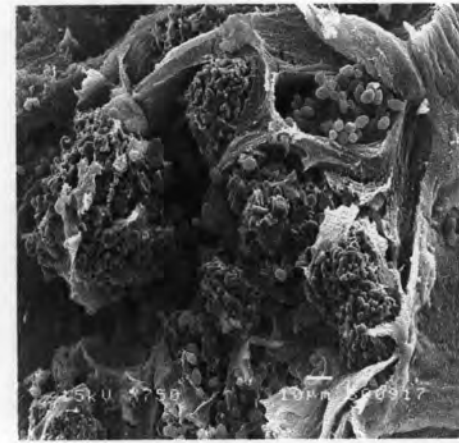


**Figure 4.42** Cross section of AEC at the end of fermentation (x750)

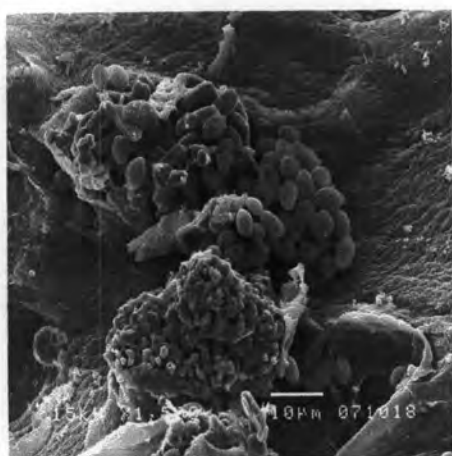


**Figure 4.43** Cross section of AEC at the beginning of fermentation (x1500)

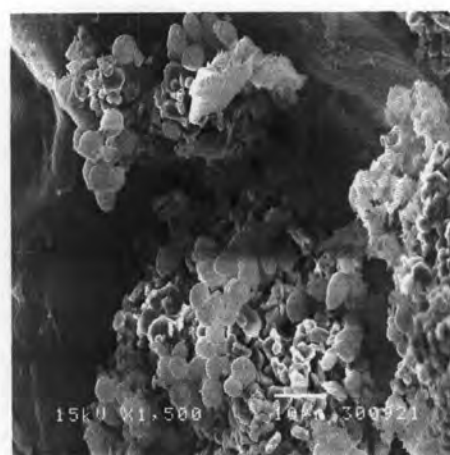


**Figure 4.44** Cross section of AEC at the end of fermentation (x1500)

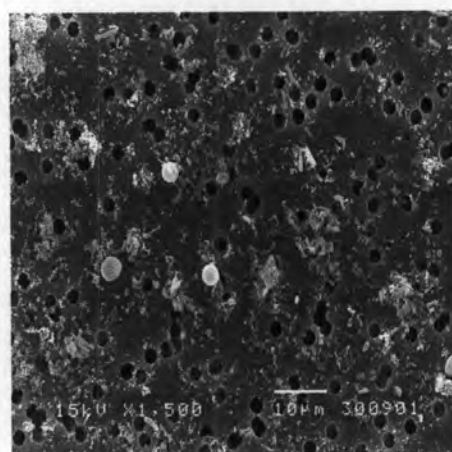


**Figure 4.45** Free cell in the effluent (x1500)

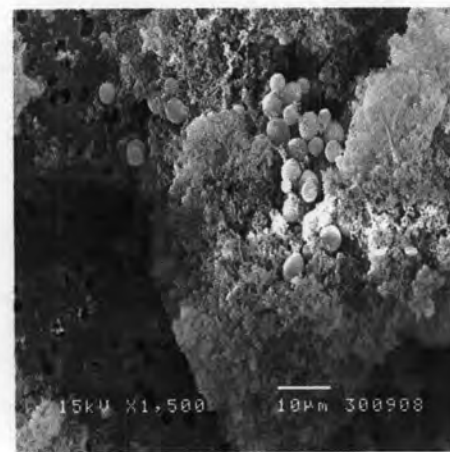


**Figure 4.46** Free cell in the reactor (x1500)

The result in the PBR demonstrated that the square shape AEC carrier was favorable for high ethanol production and stability owing to the system was operated continuously in long time (30 days) without any infection and diminution of the ethanol production. Consequently, the scale up production system by using the square shape AEC carrier with the PBR operation design is promising.